scientific reports

OPEN

Infrared thermal modulation endoscopy for label-free tumor detection

Suhyeon Kim[1,7], Gyungseok Oh[2,7], Young Ro Kim[3,4], Euiheon Chung[1,5,6] & Hyuk-Sang Kwon[1,5,6 ✉]

In optical imaging of solid tumors, signal contrasts derived from inherent tissue temperature differences have been employed to distinguish tumor masses from surrounding tissue. Moreover, with the advancement of active infrared imaging, dynamic thermal characteristics in response to exogenous thermal modulation (heating and cooling) have been proposed as novel measures of tumor assessment. Contrast factors such as the average rate of temperature changes and thermal recovery time constants have been investigated through an active thermal modulation imaging approach, yielding promising tumor characterization results in a xenograft mouse model. Here, to assess its clinical potential, we developed and deployed an endoscopic infrared thermal modulation imaging system, incorporating anti-reflection germanium lenses. Employing tissue cooling, we evaluated the feasibility of detecting in situ tumors in a syngeneic rectal tumor mouse model. Consequently, early-stage tumors were successfully localized and evaluated based on their heat signatures. Notably, tumors exhibited a higher rate of temperature change induced by thermal modulation compared to adjacent tissues. Through the introduction of this label-free technology, Infrared Thermal Modulation Endoscopy (ITME), our study showcased an effective method for optically delineating and assessing solid tumors. This innovative diagnostic technology holds significant promise for enhancing our ability to detect, classify, and characterize abnormal tissues.

For the majority of developed countries, cancer has been one of the leading causes of death, in which early detection is critically important for effective treatment[1]. Among clinically available diagnostic modalities, computerized tomography (CT) and positron emission tomography (PET) provide a highly robust means for visualizing solid tumor formation, but these methods are typically open to the risks of radiation exposure. Magnetic resonance imaging (MRI) is non-invasive but limited by high cost, relatively long acquisition time, and high sensitivity to movement. More recently, molecular imaging emerged as a novel strategy to reveal cancer-associated functional groups on tumor cells using target-specific probes designed for various imaging platforms. However, the complicated synthesis of contrast agents along with the regulation and safety issues as well as unknown distribution characteristics of these agents adds difficulties to the straightforward clinical translation of molecular imaging[2]. In this study, we address such shortcomings of current medical imaging devices and strategies through the implementation of the non-invasive, active thermal imaging technique. By utilizing dynamic heat characteristics in response to thermal modulation, we propose a label-free tumor detection method with the development of the infrared thermal modulation endoscopy (ITME), based on inherent biophysical differences between tumor and normal tissues.

For non-destructive inspection of heat signatures, thermographic imaging has been adopted as a fast, inexpensive tool to obtain visual displays of the infrared energy in an object[3]. When applied in biomedicine, infrared thermography facilitates the optical detection of solid tumors unlike other traditional tracer-based

[1]Department of Biomedical Science and Engineering, Gwangju Institute of Science and Technology, Gwangju 61005, South Korea. [2]Medical Technology Examination Division, Korean Intellectual Property Office, Daejeon 35208, South Korea. [3]Athinoula A. Martinos Center for Biomedical Imaging, Massachusetts General Hospital, Charlestown, MA 02129, USA. [4]Department of Radiology, Harvard Medical School, Boston, MA 02115, USA. [5]AI Graduate School, Gwangju Institute of Science and Technology, Gwangju 61005, South Korea. [6]Research Center for Photon Science Technology, Gwangju Institute of Science and Technology, Gwangju 61005, South Korea. [7]Suhyeon Kim and Gyungseok Oh contributed equally to this work. ✉email: hyuksang@gist.ac.kr

approaches, by precluding the administration of exogenous contrast medium into the systemic circulation. In particular, thermographic tumor identification is highly efficient due to the simplicity of the determining factor: the abnormal temperature of the tumor mass, generated by its differences in structure, physiology, and metabolism from adjacent normal tissues. Indeed, thermographic imaging has already been utilized to detect tumor formation and evaluate therapy efficacy in a breast tumor xenograft murine model[4,5]. Furthermore, transient thermal properties have been exploited via dynamic thermal imaging by assessing temporal features such as thermal relaxation time to reach the equilibrium temperature. This concept has been applied in several past studies, reporting the use of artificial surface temperature manipulation for characterizing topical tissue damage such as burn injury and melanoma skin cancer[6–8]. Additionally, external irradiation using LED enabled selective heating of red blood cells with strong absorption at 530 nm, avoiding the heating of surrounding water-rich tissue[9]. Moreover, we previously demonstrated the capability of active thermal modulation imaging to detect and analyze early-stage tumors in a xenograft murine tumor model[10].

In this study, we implemented an active endoscopic imaging modality to detect in situ rectal tumor masses in a preclinical setting to establish the practical utility of the thermal modulation technique. Tissue heating and cooling modulation were achieved using air convection. The study results demonstrate that active thermal modulation enabled the detection of early-stage tumors, which was enhanced by employing the thermal feature contrast (e.g., thermal recovery time constant). The incorporation of endoscopic features significantly improved the applicability of the thermographic imaging method, offering a potentially important way to assess and grade solid tumors based on multiple thermal characteristics. The availability of various thermal manipulation mechanisms could contribute to the methodological diversity and applicability. The current preclinical study demonstrated the capability of endoscopic thermal modulation imaging for diagnostic and prognostic evaluations of rectal tumors. Given its noninvasive feature and exclusion of an exogenous contrast medium, the clinical prospects for clinicians are noteworthy in the application of the proposed device.

Materials and methods
Development and characterization of infrared thermal modulation endoscopy (ITME)
The infrared endoscopic imaging scope consisted of a 3.0 mm insertion scope, anti-reflection (AR) - coated germanium lenses, and a thermal camera (FLIR A325sc, FLIR Systems Inc., USA) as shown in Fig. 1a. The custom-designed insertion scope was attached at the distal end of the lens tube for rectal application. The germanium
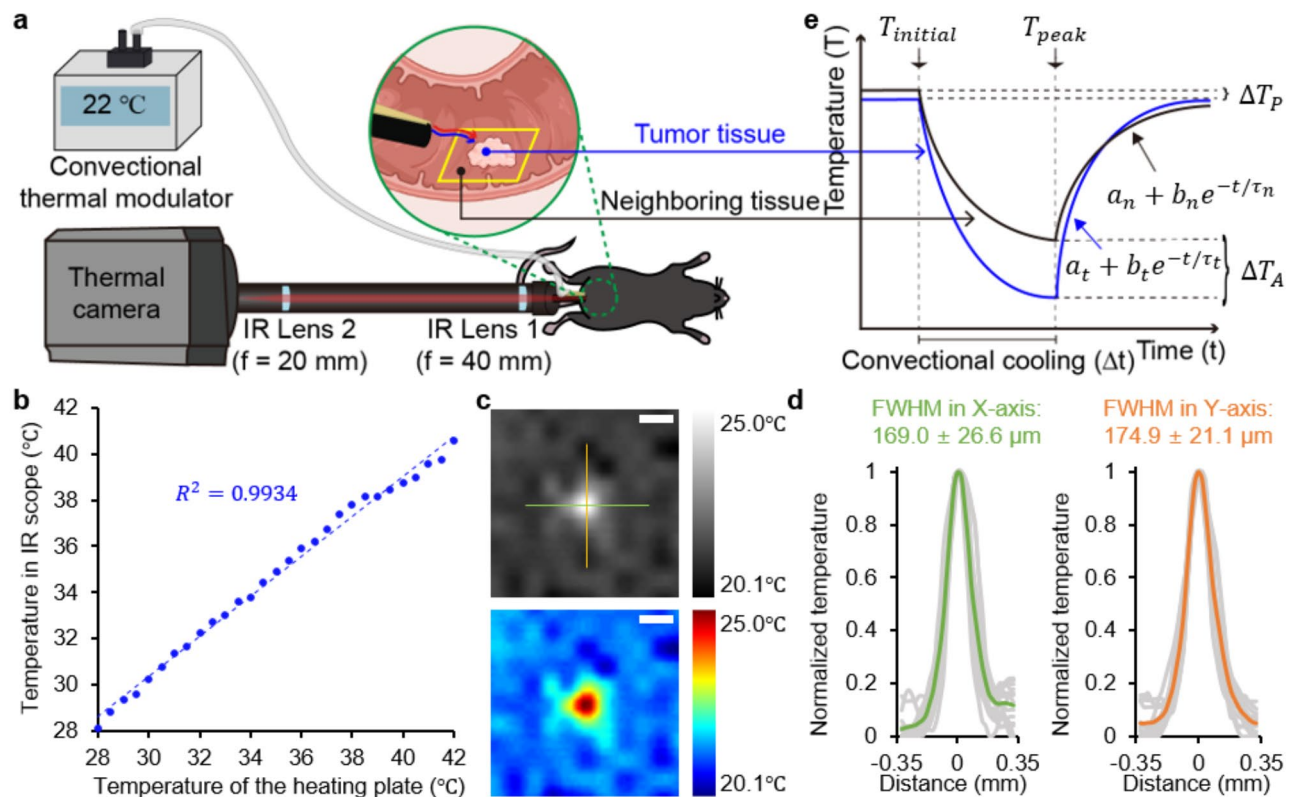

Fig. 1. Schematic of the thermal endoscopic imaging system. (**a**) The experimental setup for thermal endoscopy. (**b**) Evaluation result of the temperature sensing ability of the ITME. (**c**) IR images of the 0.1 mm pinhole attached to a heating pad. Two colormaps (gray and jet) from MATLAB are utilized. Scale bar: 0.2 mm. (d) X and Y-axis line profiles of 0.1 mm pinhole images including (c) (gray). The averaged FWHM of the X and Y-axes is calculated from 15 line profiles of each axis. (green and orange). (e) Conceptual diagram illustrating temperature changes in tumor and neighboring tissues during thermal modulation (cooling).

lens has the highest refractive index of commonly available IR–transmitters and low optical dispersion to longwave radiation. The IR light passed through the insertion scope was transmitted to the proximal end of the AR-coated germanium lenses and recorded using a thermal camera. For convectional thermal stimulation, a thermal modulator was fabricated with an air pump. Air from the thermal modulator passes through the tube and the tip (a pipet tip) connected to it. This tip is attached to the insertion scope of the endoscopy. 42 ℃ and 22 ℃ were selected for heating and cooling, respectively.

To characterize the ITME, we imaged a heating plate (LCI-0016 controlled by CU-201, Live Cell Instrument, South Korea) that underwent temperature changes from 28 °C to 42 °C. As shown in Fig. 1b, the temperature changes of the thermal endoscopic imaging system show a good linear correlation with the actual temperature changes. Additionally, the USAF 1951 resolution test target (R3L2S1P, Thorlabs, NJ, USA) and a 100 µm pinhole (P100K, Thorlabs Inc., USA) were placed on a flexible heating pad (SRFR-3/5-P, Omega Engineering Inc., United Kingdom) and imaged (Fig. S1a in Supplement file 1 and Fig. 1c). The information gleaned from the images enabled us to calculate the spatial resolution, relative contrast, and full width at half maximum (FWHM). The ITME system achieved a circular imaging field with a diameter of 5.28 mm using an insertion scope for the rectum imaging. Additionally, it attained a lateral resolution of 169.0 µm along the X-axis and 174.9 µm along the Y-axis (Fig. 1d). The uniformity of the field was assessed by plotting cross-sectional intensity profiles along the X and Y-axis. This assessment was performed using an image of a uniformly heated heating pad (Fig. S1 in Supplement file 1). The insertion scope was modeled and printed with 3D CAD software (SolidWorks 2019, SolidWorks, USA) and a 3D printer (Ultimate 2, Ultimate, England). The data were analyzed by FLIR ResearchIR MAX software (FLIR Systems Inc., USA) and MATLAB.

Tumor mouse models

SL4-DsRed, a murine colon cancer cell line was cultured to make syngeneic tumor mouse models. SL4-DsRed cancer cells were provided by the Edwin L. Steel Laboratory (Massachusetts General Hospital and Harvard Medical School, MA, USA). These cells were cultured in Dulbecco's modified Eagle's medium/Ham's F-12 (DMEM/ F12) 1:1 medium supplemented with L-glutamine and 2.438 g/L NaHCO3, 10% fetal bovine serum (FBS), 1% penicillin/streptomycin solution[11].

Six-week-old Balb/C immune-deficient female nude mice (DBL, South Korea) were used to establish the subcutaneous tumor mouse model. Each mouse received a subcutaneous injection of 1×10^6 SL4-DsRed cancer cells in 100 µL volume into the right flank tissue. The subcutaneous tumor mouse model was established following the previously described protocols[12]. In order to use the tumor in its early-stage with a volume of around 100 mm^3, tumor sizes were measured using a caliper considering an ellipsoid shape[13].

Previously, orthotopic colon cancer mouse models were established by injecting cancer cell lines into the rectal tissue[14,15]. To establish our rectal tumor mouse model, seven-week-old C57BL/6 mice were used. While under anesthesia in a supine position, mice underwent gentle anal dilation using blunt-tripped forceps at the anal opening. A 30-gauge syringe was then used to inject 1×10^6 SL4 cancer cells labelled red fluorescent protein in PBS submucosally into the distal posterior rectum. The injection site was at the rectal mucosa, approximately 1–2 mm beyond the anal canal. Mice were observed for 2 h until fully recovered and monitored twice weekly for tumor development[16].

Label-free tumor imaging was performed when the tumor was in its early-stage (< 100 mm^3) considering the aim of early detection of the tumor. Following the implantation of SL4-DsRed cancer cells, endoscopic imaging was conducted twice a week to monitor tumor formation through red fluorescence. Throughout all experiments, including surgery and imaging, the mice were kept anesthetized. We intraperitoneally administered a Zoletil/ Xylazine (60/10 mg/kg body weight) mixture diluted with saline solution.

The study commenced in October 2021 following the approval from the Institute Animal Care and Use Committee (IACUC) of Gwangju Institute Science and Technology (GIST) under the protocol number GIST-2021-103. All procedures, including animal handling, were conducted in strict accordance with IACUC guidelines and the ARRIVE guidelines. Mice were housed in a controlled environment under a 12-hour light/ dark cycle with unlimited access to food and water. They were monitored daily for signs of distress or discomfort, including abnormal behavior or pain. If any criteria for suffering were met, they were humanely euthanized using CO_2 inhalation, as permitted by IACUC guidelines, to ensure death.

Active thermal modulation measurement in subcutaneous and rectal tumor mouse models

Thermal imaging experiments were conducted at a constant room temperature (22 ± 1 ℃). During the investigation, ambient lighting was minimized to avoid affecting the performance of the thermal camera. First, the steady-state temperature distribution in the tumor and neighboring tissues was recorded for 10 s using the thermal camera (passive thermal imaging). Subsequently, external thermal modulation was applied while measuring temperature changes from the tissue surface for 10 s (i.e., active thermal imaging). The goal of thermal modulation was to alter the temperature of the skin surface sufficiently to induce a transient thermal response, thereby differentiating the tumor from the neighboring tissues. After the convectional thermal modulation, the tissue temperature was recorded as it returned to its background level over 40 s (i.e., recovery phase). Finally, the time series of thermal images were quantitatively assessed to extract the rate of temperature change and thermal recovery time constant.

In the study with the subcutaneous model, we used convectional modulation to enhance the thermal contrast. Either warm or cool air at 42 ℃ or 22 ℃, respectively, was blown onto the flank, including the tumor area for 10 s with an airflow velocity of 3.6 m/s. With the rectal models, we similarly employed convectional cooling, in which cool air at 22 ℃ was blown onto the rectum tissue including the tumor area. As previous study has shown that tissue damage can begin at 43 ℃[17], only the cooling modulation was used in the mouse rectum to avoid potential tissue damage due to temperature increase in the enclosed space. From each group (subcutaneous and rectal

tumor models), three mice were used with the active thermal modulation measurement repeated 3–4 times per mouse. All experiments were conducted within three weeks of implantation before the tumor became too large.

In addition to the developed endoscope, a customized fluorescence imaging system was used to locate the tumor cells labelled with red fluorescent protein after thermal modulation imaging for confirmation. Specific details of the fluorescence endoscopy are described in the literature[18]. After the localization of the tumor, we then collected thermal data related to early-stage tumors in the same tumor mouse models. These data were processed using FLIR ResearchIR Max software, (FLIR Systems, Inc., USA). After post-processing, temperatures of neighboring and tumor tissues were plotted over time to evaluate thermodynamic modulation. The raw image data were analyzed using OriginPro software (OriginLab Corporation, Northampton, MA, USA) to visualize and examine the time series of temperature changes in the selected region of interest.

Quantification of active thermal contrast parameters

From the diagram of temperature changes in tumor tissue and neighboring tissue over time, we calculated the rate of temperature change and the thermal recovery time constant to quantify the thermodynamic contrast. In addition, we measured the temperature difference between the tumor and neighboring tissues using both active and passive thermal imaging, with and without convectional thermal modulation, respectively. From Fig. 1e, the rate of temperature change ($℃$/sec) represents the average rate of temperature change during the convectional thermal modulation ($\frac{T_{peak} - T_{initial}}{\Delta t}$), calculated separately for the tumor and neighboring tissue. The thermal recovery time constant (τ) was determined using the simple exponential fitting ($T(t) = a + be^{-t/\tau}$) in OriginPro software. The temperature differences between the tumor and neighboring tissue were obtained before and after the convectional thermal modulation, for either passive (ΔT_P : $T_{initial}$ difference) or active thermal imaging (ΔT_A : T_{peak} difference), respectively. For the temperature difference, values averaged the results of three mice in a group were used for the analysis.

Experimental results

To examine the utility of the ITME, we additionally took visible data using white-light and fluorescence imaging in the mouse tumor model to confirm the presence of tumor tissue. The active thermal modulation measurement consists of three phases: (1) the initial stage when the surface temperature is in equilibrium with the ambient condition, (2) the heating or cooling phase during active thermal modulation, and (3) the thermal recovery phase without thermal modulation. During thermal imaging, distinct thermal responses were observed in temperature changes in tumors and adjacent tissues throughout the manipulation and recovery phase. The results indicate that the external thermal modulation can effectively enhance the temperature contrast between the tumor and neighboring tissues. The time courses of tissue temperature during convectional heating and cooling processes were plotted and compared, where notable differences in thermal traits were observed between the tumor and neighboring tissues. In particular for the rectal model, the thermal endoscope with a scope diameter of 3 mm was inserted into the mouse rectum, in which the same active thermal imaging was performed for the cooling modulation.

Active thermal modulation measurement in subcutaneous tumor mouse model

Subsequent to tumor identification via white-light and fluorescence imaging, we performed active thermal imaging at the frame rate of 15 Hz, chosen for optimal temporal resolution, on a subcutaneous tumor mouse model (Fig. 2a-b). The temperature of tumor tissues increased more rapidly than that of surrounding tissues during the heating phase (Fig. 2c-d), and conversely, decreased more sharply during the cooling phase (Fig. 2e-f). The maximal temperature contrast between the tumor and adjacent tissues was observed at the 20-second mark for both heating and cooling. Average data from quadruplicate experiments indicate that this thermal contrast can be accentuated by applying thermal modulation, bolstering the detection capabilities of our method (Fig. 2c, e). Representative thermal images showcasing the efficacy of tumor detection at various intervals (0, 20, and 60 s) during each modulation phase are provided (Fig. 2d, f), indicating the potential of our active thermal modulation approach for improved tumor visualization.

Quantification of active thermal imaging parameters in subcutaneous tumor mouse model

As depicted in Fig. 3, the active application of heating and cooling stimuli revealed that thermal contrast parameters, such as the rate of temperature change and the thermal recovery time constant, displayed a significant difference between the tumor and neighboring tissues. Specifically, in xenograft subcutaneous tumors utilizing heating modulation, we found that the rate of temperature increase in tumor tissue (0.68 ± 0.07 $℃$ = 8.05 ± 0.87) compared to its neighboring tissue (0.49 ± 0.04 $℃$/sec and $\tau_N = 10.47 \pm 0.57$), as depicted in Fig. 3a-b. Similarly, with cooling modulation, the rate of temperature decrease in tumor tissue was greater (-0.40 ± 0.07 $℃$/sec) than that in the neighboring tissue (-0.27 ± 0.03 $℃$/sec), and the thermal recovery time constant was smaller for the tumor tissue ($\tau_T = 8.63 \pm 0.81$) compared to the neighboring tissue ($\tau_N = 10.34 \pm 0.81$), as shown in Fig. 3d-e. In summary, the temperature modulation was more rapid in the tumor area than in the neighboring tissue. Moreover, the temperature differentials between the tumor and adjacent tissue obtained from the active thermal imaging were larger than those from passive thermal imaging for both heating and cooling modulations (Fig. 3c, f). These findings demonstrate that convectional thermal modulation can induce a transient thermal response, facilitating the differentiation between the tumor and neighboring tissues. All comparative results showed statistical significance ($p < 0.01$), which was similarly and consistently observed in early-stage tumors.
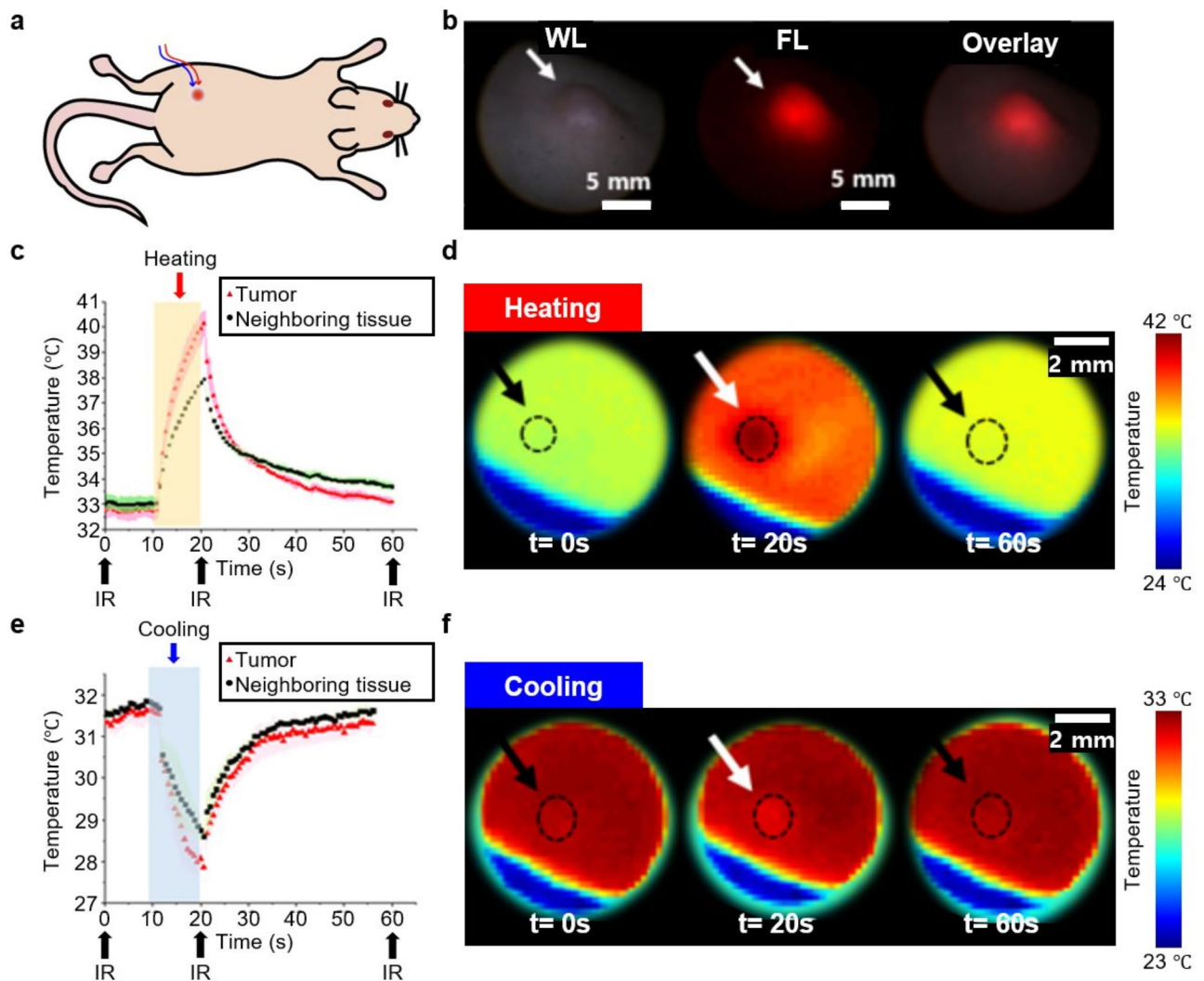
Fig. 2. Thermal contrast imaging using convectional thermal modulation on a subcutaneous tumor mouse model. (**a**) Schematic representation of imaging subcutaneous tumor mouse model. (**b**) Comparative visualization of the tumor under white-light (WL) imaging, fluorescence (FL) imaging, and their superimposed image. (**c**)-(**d**) IR imaging results during convectional heating. (**c**) Temperature dynamics in the tumor versus neighboring tissue over time during heating. (**d**) Sequential IR images captured at 0, 20, and 60 s, showing temperature distribution. (**e**)-(**f**) IR thermal imaging results during convectional cooling. (**e**) Temperature dynamics over time in tumor and neighboring areas during cooling. (**f**) IR images showing the cooling process recorded at the same intervals as heating.

Active thermal modulation measurement and quantitative analysis in rectal tumor mouse model

A syngeneic rectal tumor mouse model, induced by SL4-DsRed cancer cells, was established (Fig. 4a). Prior to thermal imaging, we utilized a home-built imaging system to locate grossly visible tumors within the mouse rectum (Fig. 4b). Passive thermal imaging failed to discern tumor formation due to the minimal thermal contrast between the tumor and neighboring tissues. Consequently, a 10-second convectional thermal modulation was applied during a 60-second imaging period, similar to the previous experiment, by directing cool air into the mouse's rectum (Fig. 4c). During the modulation phase, the tumor region's temperature decreased more rapidly than the neighboring areas.

Sequential thermal endoscopic images revealed the greatest temperature difference between the tumor and neighboring tissues at the 20-second mark following the end of cooling modulation (Fig. 4d). This substantial temperature disparity persisted throughout the thermal recovery phase, indicating that the cooling process augmented the thermal contrast between the tumor and normal tissues. Under appropriate conditions, thermal IR imaging can effectively distinguish between the thermal radiations from the tumor and neighboring tissues.

As depicted in Fig. 4e-f, the tumor tissue exhibited a greater rate of temperature decrease (-0.28 ± 0.03 ℃/sec) and a shorter thermal recovery time constant ($\tau_T = 8.76 \pm 0.30$) compared to the neighboring tissue (-0.20 ± 0.02 ℃/sec and $\tau_N = 10.49 \pm 0.60$) under cooling modulation. In essence, temperature modulation
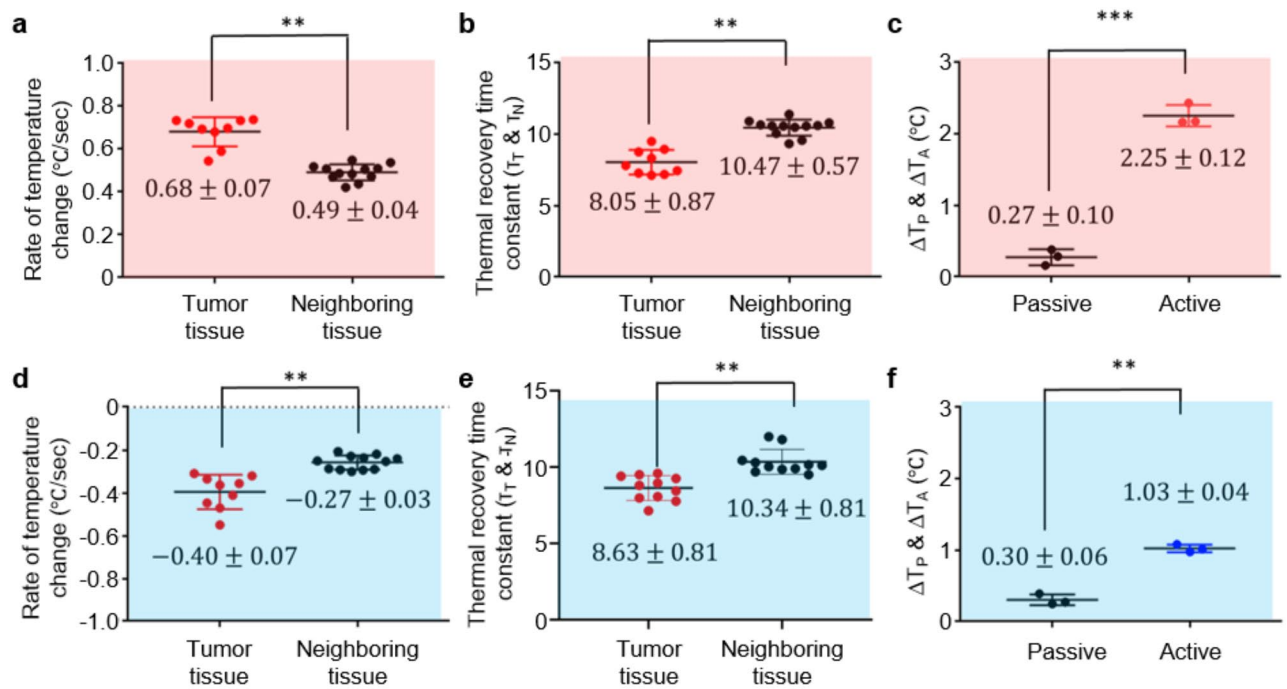
Fig. 3. Quantitative analysis of thermal contrast parameters in subcutaneous tumor model. The parameters were obtained through convectional heating (**a**-**c**) and cooling (**d**-**f**) modulation. Panels (**a**) and (**d**) display the rate of temperature changes in the tumor and neighboring tissue during thermal modulation. Panels (**b**) and (**e**) show the thermal recovery time constants for tumor (τ_T) and neighboring tissues (τ_N) post-modulation. Panels (**c**) and (**f**) compare the temperature differentials between tumor and neighboring tissues during passive (ΔT_P) and active (ΔT_A) thermal imaging. Error bars represent standard deviations calculated from all ROI data. Statistical significance is denoted as follows: ** indicates $p < 0.01$ and *** indicates $p < 0.001$.

occurred more swiftly in the tumor region than in the neighboring tissue, and the thermal recovery of the tumor tissue was faster post-cooling modulation. Furthermore, the active thermal imaging demonstrated a larger temperature difference ($\Delta T_A = 1.18 \pm 0.30$ ℃) between the tumor and neighboring tissue obtained than did the passive thermal imaging ($\Delta T_P = 0.53 \pm 0.27$ ℃) during cooling modulation (Fig. 4g).

Heating modulation was not conducted in the rectal tumor model to avoid the risk of internal tissue damage from hot air accumulation.

Discussion

In this study, we pioneered an Infrared Thermal Modulation Endoscopy (ITME) technique to distinguish tumor tissue from adjacent tissue based on dynamic thermal response. By integrating extrinsic thermal modulators into thermal endoscopy, we have engineered active thermal imaging as an effective label-free tool for tumor detection. Our study focused on leveraging the benefits of active dynamic thermal imaging to artificially heighten the thermal signal contrast, a stark departure from the reliance of passive thermal imaging on subtle temperature differentials between tumors and surrounding tissues. In the current investigation, employing both subcutaneous and rectal tumor mouse models, we have showcased the proficiency of active thermal imaging in pinpointing early-stage tumors. Experimentally, to substantiate the efficacy of active thermal IR imaging, we corroborated the tumor tissue locations using both white-light and fluorescence imaging modalities in conjunction with ITME within an in vivo setting. Of particular significance is our demonstration of the potential of integrating infrared endoscopy with thermal modulators for in situ rectal tumor detection. The current findings underscore the practicality of our approach, which employed controlled convective heating and/or cooling strategies.

Tumor tissue typically exhibit distinctive physiological and architectural traits compared to normal tissue, particularly in relation to blood vessels. The blood vessels in tumors often display a diminished caliber and irregular arrangement, resulting in compromised blood flow and drainage[19]. Both the baseline blood flow and the vascular response to thermal stimuli likely influence the dynamic thermal response traits in tumors. Under heat exposure, normal blood vessels dilate to dissipate excessive heat from the tissue[20]. Consequently, during both heating and cooling phases, variations in basal vascular state and heat dissipation mechanism likely results in variable thermal recovery time constants across normal and tumor tissue types. In addition, our experiments indicated that, at steady-state, the temperature of tumor tissue in both subcutaneous and rectal tumor mouse models is generally lower compared to that of adjacent tissues, a phenomenon potentially influenced by altered blood flow and thermoregulatory mechanisms. Employing these intrinsic differences in thermos-vascular characteristics, we devised an external means to amplify the thermal contrast by directly applying thermal stress to the tumor tissue. We further hypothesize that active thermal imaging results demonstrate significant image
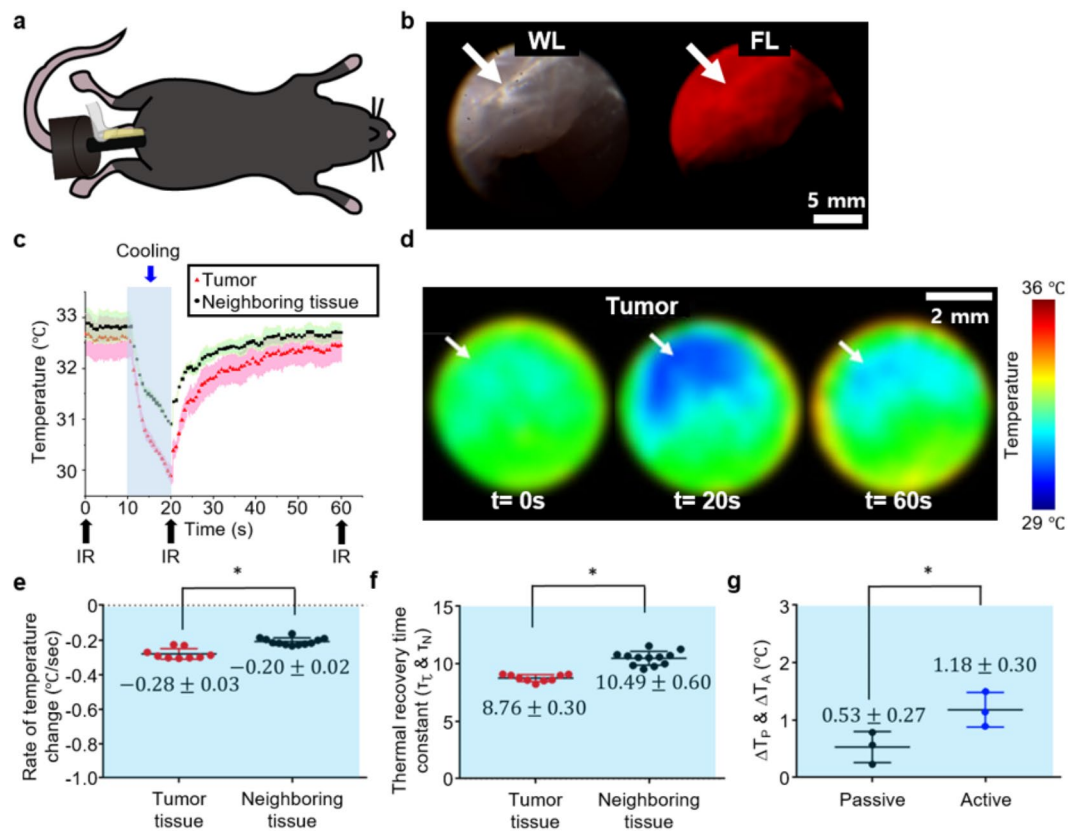
Fig. 4. Assessment of thermal modulation imaging with convectional cooling to detect early-stage mouse rectal tumors. (**a**) Schematic of the imaging procedure for a rectal tumor in a mouse. (**b**) Visual differentiation of the tumor under white-light (WL) and fluorescence (FL) imaging. (**c**)-(**d**) IR imaging results following convectional cooling: (**c**) Temperature trajectories in tumor and neighboring tissues during cooling. (**d**) IR images captured at 0, 20, and 60 s, illustrating temporal thermal changes. (**e**)-(**g**) Quantitative analysis of the thermal contrast parameters: (**e**) The rate of temperature changes. (**f**) The thermal recovery time constants for tumor (τ_T) and neighboring tissues (τ_N) post-thermal modulation. (**g**) Differential temperature analysis between tumor and neighboring tissues under passive (ΔT_P) and active (ΔT_A) thermal conditions. Error bars represent standard deviations from all the ROI data. Statistical significance is denoted by *: $p < 0.05$.

contrast based on thermos-physical properties, such as the rate of temperature change and thermal recovery time constant, effectively delineating the solid tumor mass.

Typically, body temperature varies gradually, with the skin temperatures adjusting rapidly to ambient changes, followed by the more gradual responses of deeper tissues. The regulation of blood flow is essential in this thermoregulation. Ectopically implanted tumor models are often display reduced vascular density[21], contributing to lower rates of blood flow changes in tumors compared to normal tissue altering thermoregulatory responses. Variations in blood flow, blood volume, and tissue composition also give rise to the distinct thermal characteristics observed between tumor and normal tissues. Furthermore, the potential for inadequate development of peripheral nerves within tumor tissue could exacerbate these differences, as effective thermoregulation relies on an internal feedback mechanism that detects and adjusts to local temperature fluctuations to maintain thermal homeostasis[10]. Consequently, our results suggest that tumor tissue warms up more rapidly during heating modulation due to localized heat accumulation, which cannot be dissipated effectively by blood flow. Similarly, cooling occurs faster in tumor tissue compared to surrounding tissues, due to the tumor's diminished capacity to counteract heat loss during cooling modulation.

During the thermal recovery phase, tumor tissue temperatures changed more rapidly than those of the surrounding tissue, despite the tumor's compromised thermoregulatory capacity. To investigate whether the atypical thermal responses of tumors arise from differences in intrinsic tissue compositions or vascular structure compared to adjacent tissue, we analyzed ex vivo specimens from a subcutaneous tumor in a mouse model (see Fig. S2 in Supplement file 1). In the absence of blood flow, tumor tissue demonstrated a more pronounced temperature increase upon heating compared to normal tissue. Our experiments indicated that tumor tissue's thermal response to external thermal modulation is distinct from that of surrounding tissue, contributing to an increased thermal contrast. Employing the ITME system, which offers simultaneous convective thermal modulation and thermal imaging, we were able to effectively differentiate tumor tissue.

While the infrared spectrum is useful for diagnostic applications in dermatology, the primary challenge with thermal imaging is its limited penetration depth, typically up to 2–3 mm[22]. Moreover, imaging can be

compromised by movement artifacts from respiration and heartbeat, affecting the precision of temperature measurements. Minor movements of the animals during convective modulation also have affected image quality. In future studies, a motion compensation method will be employed to accurately align images taken at different times, allowing for a more precise measure of temperature distribution during thermal recovery. In addition, thermal stimulation using an IR light source could replace convectional stimulation, offering more sophisticated stimulation control in both models. While this approach cannot be used for cooling, radiative heating could be effectively utilized in thermal modulation endoscopy, enabling heating stimulation for the rectal tumor model. These improvements will mitigate data variability and enhance overall data quality.

Conclusions
In conclusion, this study marks substantial advancements in the use of mouse tumor models. Our methodology applies 'convection mode' thermal modulation for label-free tumor detection, thereby improving thermal contrast. Furthermore, we have executed the detection of rectal tumors within the gastrointestinal tract using active convective cooling, contributing to a more complete understanding of the varied thermal responses between tumor tissue and its neighboring tissue.

Data availability
The data underlying the results presented in this paper are not publicly available at this time but may be obtained from the corresponding authors upon reasonable request.

References
1. López-Gómez, M., Malmierca, E., de Górgolas, M. & Casado, E. Cancer in developing countries: the next most preventable pandemic. The global problem of cancer. *Critical reviews in oncology/hematology* 88, 117–122 (2013).
2. Weissleder, R. & Pittet, M. J. Imaging in the era of molecular oncology. *Nature*. **452**, 580 (2008).
3. Chen, W. Thermometry and interpretation of body temperature. *Biomed. Eng. Lett.* **9**, 3–17 (2019).
4. Song, C. et al. Thermographic assessment of tumor growth in mouse xenografts. *Int. J. Cancer*. **121**, 1055–1058 (2007).
5. Hussain, N. et al. The use of thermographic imaging to evaluate therapeutic response in human tumour xenograft models. *Sci. Rep.* **6**, 31136 (2016).
6. Herman, C. The role of dynamic infrared imaging in melanoma diagnosis. *Expert Rev. Dermatology*. **8**, 177–184 (2013).
7. Renkielska, A. et al. Active dynamic infrared thermal imaging in burn depth evaluation. *J. Burn Care Res.* **35**, e294–e303 (2014).
8. Godoy, S. E. et al. Detection theory for accurate and non-invasive skin cancer diagnosis using dynamic thermal imaging. *Biomed. Opt. Express*. **8**, 2301–2323 (2017).
9. Case, J. R., Young, M. A., Dréau, D. & Trammell, S. R. Noninvasive enhanced mid-IR imaging of breast cancer development in vivo. *J. Biomed. Opt.* **20**, 116003 (2015).
10. Oh, G., Lee, K. H. & Chung, E. Active thermodynamic contrast imaging for label-free tumor detection in a murine xenograft tumor model. *Biomed. Opt. Express*. **8**, 5013–5026 (2017).
11. Yoo, S. W. et al. Endoscopic non-ablative fractional laser therapy in an orthotopic colon tumour model. *Sci. Rep.* **8**, 1673 (2018).
12. Yoo, S. W. et al. Non-ablative fractional thulium laser irradiation suppresses early tumor growth. *Curr. Opt. Photonics*. **1**, 51–59 (2017).
13. Sápi, J. et al. Tumor volume estimation and quasi-continuous administration for most effective bevacizumab therapy. *PLoS One*. **10**, e0142190 (2015).
14. Donigan, M. et al. Novel murine model for colon cancer: non-operative trans-anal rectal injection. *J. Surg. Res.* **154**, 299–303 (2009).
15. Kishimoto, H. et al. Development of a clinically-precise mouse model of rectal cancer. *PLoS One*. **8**, e79453 (2013).
16. Kim, M. P. et al. Generation of orthotopic and heterotopic human pancreatic cancer xenografts in immunodeficient mice. *Nat. Protoc.* **4**, 1670 (2009).
17. Martin, N. & Falder, S. A review of the evidence for threshold of burn injury. *Burns*. **43**, 1624–1639 (2017).
18. Oh, G. et al. Intravital imaging of mouse colonic adenoma using MMP-based molecular probes with multi-channel fluorescence endoscopy. *Biomed. Opt. Express*. **5**, 1677–1689 (2014).
19. Siemann, D. W. The unique characteristics of tumor vasculature and preclinical evidence for its selective disruption by tumor-vascular disrupting agents. *Cancer Treat. Rev.* **37**, 63–74 (2011).
20. Horsman, M. R. Tissue physiology and the response to heat. *Int. J. Hyperth.* **22**, 197–203 (2006).
21. Ho, K. S., Poon, P. C., Owen, S. C. & Shoichet, M. S. Blood vessel hyperpermeability and pathophysiology in human tumour xenograft models of breast cancer: a comparison of ectopic and orthotopic tumours. *BMC cancer*. **12**, 579 (2012).
22. Gurjarpadhye, A. A., Parekh, M. B., Dubnika, A., Rajadas, J. & Inayathullah, M. Infrared imaging tools for diagnostic applications in dermatology. *SM J. Clin. Med. Imaging*. **1**, 1 (2015).

Author contributions
E.C. and H.K. conceived the project. S.K. and G.O. performed experiments, analyzed the data, and wrote initial drafts. E.C., H.K., and Y.K. interpreted the data and contributed to writing the manuscript. All authors read and approved the final manuscript.

Declarations

Competing interests
The authors declare no competing interests.

Supplementary information
See Supplement file 1 for supporting content.

Additional information
Supplementary Information The online version contains supplementary material available at https://doi.org/10.1038/s41598-024-76173-8.

Correspondence and requests for materials should be addressed to H.-S.K.

Reprints and permissions information is available at www.nature.com/reprints.

Publisher's note Springer Nature remains neutral with regard to jurisdictional claims in published maps and institutional affiliations.